Giant oscillations in a magneto-optical trap

Andrea di Stefano, Marie Fauquembergue, Philippe Verkerk, and Daniel Hennequin
Laboratoire de Physique des Lasers, Atomes et Molécules, UMR CNRS, Centre d'Etudes et de Recherches Lasers et Applications, Université des Sciences et Technologies de Lille, F-59655 Villeneuve d'Ascq Cedex, France

(Received 11 February 2002; published 21 March 2003)

The present paper reports on the study of deterministic instabilities in the atomic cloud of a magneto-optical trap. Giant periodic and erratic self-oscillations are experimentally observed and analyzed through a simple original model taking into account the shadow effect and the spatial distribution of the atoms in the cloud. We show that giant oscillations are induced by a homoclinic orbit merging in the neighborhood of a Hopf bifurcation.

DOI: 10.1103/PhysRevA.67.033404 PACS number(s): 32.80.Pj, 05.45.-a

The magneto-optical cooling of atoms is at the origin of a renewal of atomic physics. It is used in various fields, such as Bose-Einstein condensates [1], optical lattices [2], and quantum chaos [3], and could lead to several applications, such as atomic clocks [4] or quantum computing [5]. Although the technology and realization of magneto-optical traps (MOT) is well mastered, some experimental adjustments remain empirical. It is, in particular, well known by experimentalists that, for dense atomic clouds close to resonance, instabilities appear in the spatiotemporal distribution of the atoms. This problem is usually fixed by slightly misaligning the trapping beams.

A recent study has concluded that the so-called instabilities are not really instabilities, but originate in the amplification of experimental noise through coherent resonance [6]. It also showed the main role of the shadow effect: because of the absorption of light inside the cloud, the intensities of the backward and forward beams are locally different, leading to an internal attractive force. In the configuration where each backward beam is obtained by retroreflection of the forward beam, the symmetry between forward and backward beams is broken, and an external force appears, displacing the cloud along the bisectors of the trap beams.

We report here the experimental observation of actual instabilities, consisting in giant oscillations of the cloud. This large amplitude motion is periodic or erratic, depending on the parameters. A modified version of the model developed in Ref. [6] allows us to describe the mechanisms at the origin of the giant oscillations, through a stability analysis of the stationary and dynamical solutions, in particular in the vicinity of a Hopf bifurcation [7]. This approach, adopted, to our knowledge, for the first time in this domain, confirms the existence of deterministic instabilities in the MOT.

The experimental setup is a standard three-arm σ^+-σ^- MOT on cesium [6]. In each arm, the beam is retroreflected, creating an intensity asymmetry that generates a center-of-mass motion. Note that this choice is not restrictive, as it simply links the local motion inside the cloud to a global motion, easily detected with a crossed couple of four-quadrant photodiodes. This motion is recorded through the location z of the center of mass, complemented by the number of atoms n in the cloud. The trap beam waist is 3 mm, and the forward and backward beams are carefully aligned. The magnetic field gradient is 13 G/cm. The main change with respect to the experiment described in Ref. [6] is a larger laser intensity, up to $I_1 = 20$ mW/cm^2 per beam.

A typical experiment consists in recording the dynamics for fixed parameters, and repeating the measurement for different values of the detuning Δ_0 between the trap laser beams and the atomic transition, without changing the other parameters. Far from resonance, the cloud is stable. When the resonance is approached, the behavior becomes abruptly unstable for $\Delta_0 = -1.7$ (Δ_0 is in units of the natural width Γ of the atomic transition). The resulting periodic oscillation, which we call C_A, appears as an asymmetric cycle, with a slow growth of both z and n followed by a fast stage, where n decreases (Fig. 1). The characteristic times of the growth and loss stages differ by more than one order of magnitude. But the most striking feature of our observations was the amplitude of the spatial oscillations, which can be more than 100 times greater than those reported in Ref. [6]. This behavior depends of course on the parameters, but not in a critical way. For example, increasing the beam intensity simply shifts the bifurcation points, without changing the shape of the dynamics.

Figure 2 shows, for an intensity larger than that in Fig. 1, the evolution of the frequency ω of the oscillations when Δ_0 is changed: far from resonance, ω is constant. For $\Delta_0 \simeq$

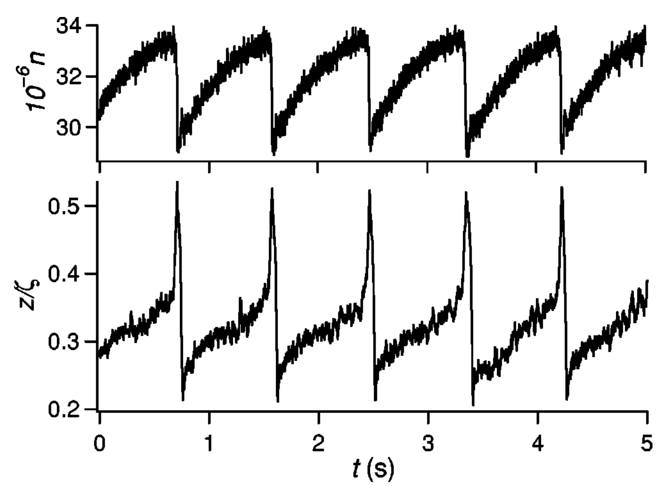

FIG. 1. Experimental record of a C_A periodic instability. Parameters are $I_1 = 11$ mW/cm^2 and $\Delta_0 = -1.4$. ζ is the size of the cloud. Here $\zeta \simeq 3$ mm.

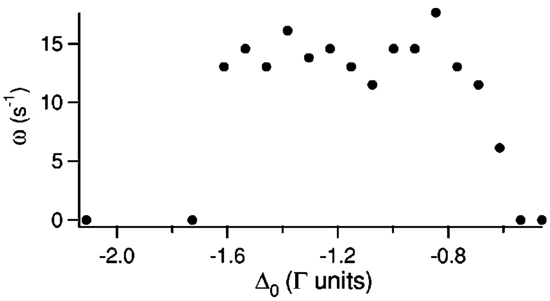

FIG. 2. Evolution of the instability frequency ω vs the detuning for $I_1 = 20$ mW/cm^2.

-0.8, the behavior changes: the global shape of the oscillations remains the same, alternateing between slow and fast variations of z and n (Fig. 3). But the periodicity has disappeared, and the return time τ of the dynamics is erratic. For $\Delta_0 > -0.8$, Fig. 2 reports the mean value of $2\pi\tau^{-1}$, which decreases drastically with Δ_0. An analysis of τ with the usual techniques of nonlinear dynamics (Poincaré section, first return time diagram) does not put in evidence any order, and our conclusion is that the irregularity of these instabilities, which we call C_B, originates in noise and is not deterministic chaos. Finally, for $\Delta_0 > -0.55$, the instabilities disappear and the behavior is again stationary.

To understand the origin of these giant oscillations, we use the one-dimensional (1D) model introduced in Ref. [6]. The system is modeled through the equations of motion of z and a rate equation of n. We have:

$$\frac{d^2 z}{dt^2} = \frac{1}{M} F_T, \tag{1a}$$

$$\frac{dn}{dt} = B(n_e - n), \tag{1b}$$

where M is the mass of the cloud, F_T is the total external force, n_e is the atom number at equilibrium, and B is the population relaxation rate. n_e is assumed to depend on z, to take into account the depopulation of the cloud outside the trap center. We define a distance z_0, linked to the trap beam waists, beyond which the trap is empty ($n_e = 0$). For $z < z_0$, we assume a quadratic behavior $n_e = n_0[1-(z/z_0)^2[$, where n_0 is the cloud population at the trap center.

To take into account the shadow effect, the model in Ref. [6] considered the cloud as a point object, and so was valid only for small clouds in the vicinity of $z=0$. Indeed, when the cloud approaches z_0, the border affects the cloud progressively, in proportion to the number of atoms located beyond z_0. Thus the cloud spatial distribution becomes crucial for giant oscillations, such as those observed here. To model it, we consider that, starting from an input forward intensity I_1, the intensity after a first crossing of the cloud (i.e., the input backward intensity) is $I_2 < I_1$, and the remaining intensity after a second crossing of the cloud (i.e., the output backward intensity) is $I_3 < I_2$. The rate of photons absorbed in the forward [backward] beam is $S(I_1 - I_2)/h\nu$ [$S(I_2 - I_3)/h\nu$], where S is the cross-sectional area of the cloud and $h\nu$ the energy of a photon. The force associated with each beam is the product of the number of absorbed photons and the elementary momentum $\hbar k$,

$$F_T = \frac{S}{c}(I_1 - 2I_2 + I_3). \tag{2}$$

To get a relation between I_1, I_2, and I_3, we solve the equations of propagation of the two beams through the atomic cloud. Since the MOT is operated with high intensity beams and small detunings, a Doppler model is suitable and we can assume a $J=0 \rightarrow J=1$ transition. Inside the cloud, the intensity I_+ (I_-) of the σ_+ (σ_-) forward (backward) polarized beam evolves due to photon scattering, which is proportional to the corresponding excited-state populations $\Pi_\pm$. The evolution equations of the intensity are simply

$$\frac{dI_\pm}{dz} = \mp \Gamma h\nu\rho\Pi_\pm, \tag{3}$$

where ρ is the atomic density in the cloud. The populations $\Pi_\pm$ are given by the steady state of the master equation. The underlying hypothesis is that the evolution of the external degrees of freedom is much slower than that of the internal ones. The populations $\Pi_\pm$ depend on both I_+ and I_-, so that Eq. (3) is a set of coupled nonlinear equations. They are integrated numerically from the side of the cloud where $I_+ = I_- = I_2$, to the other side, where $I_- = I_3$ and $I_+ = I_1$, assuming that the density ρ is constant, because of multiple scattering [8]. Note that this method to treat absorption also properly takes into account the cross saturation, contrary to the model in Ref. [6].

When Δ_0 is varied as in the experiment, the stationary solutions exhibit two sudden changes of the slope, leading to a "fold" in the parameter space [Fig. 4(a)], as in Ref. [6]. The slope of the fold depends on the other parameters (e.g., n_0), evolving from a flat dependence to bistability. Far from bistability, the stationary solutions are stable everywhere, including the fold: in this case, the model is equivalent to that

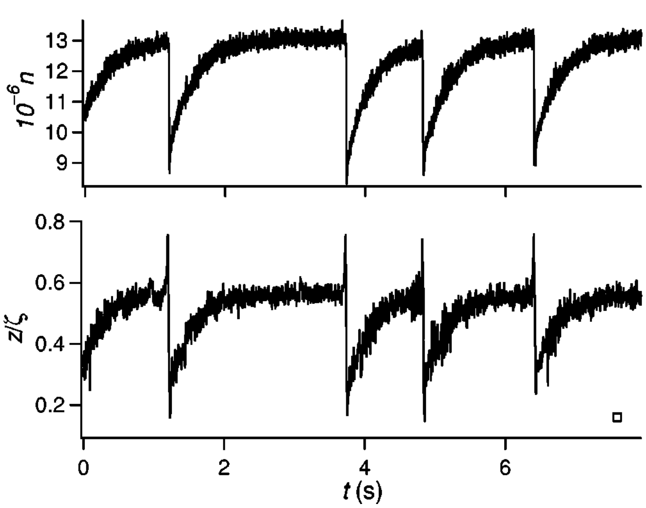

FIG. 3. Experimental record of a C_B-like instability. Parameters are the same as in Fig. 2 with $\Delta_0 = -0.6$. $\zeta \simeq 5$ mm.

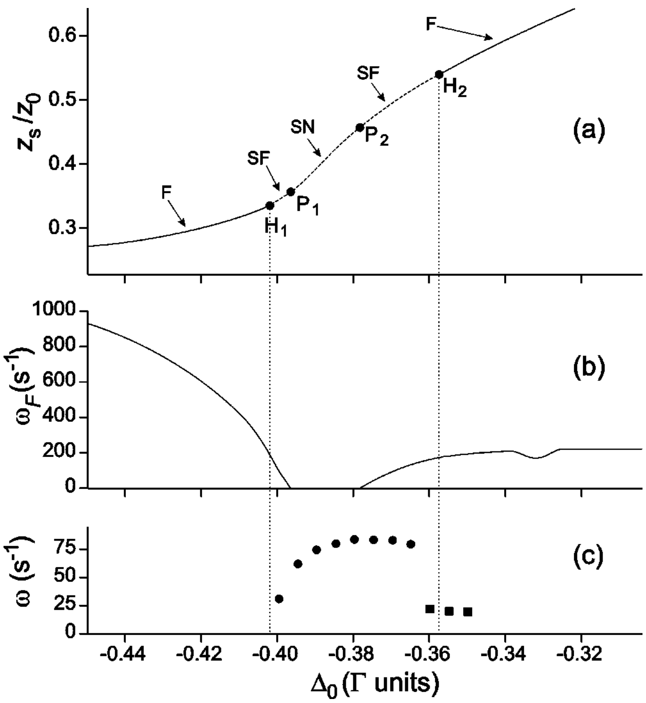

FIG. 4. Theoretical evolution of the behavior of the cloud as a function of the detuning. In (a), the stationary solution z_s of z is stable (full line) or unstable (dashed line). At points H_1 and H_2, a Hopf bifurcation occurs, while at points P_1 and P_2, ω_F vanishes. F (focus), SF (saddle focus), and SN (saddle node) refer to the nature of the fixed point representing the stationary solution in the phase space. (b) Evolution of ω_F vs Δ_0. (c) Plot of the instability frequencies ω_A (circles) and ω_B (squares). Parameters for the calculations are $I_1=33$ mW/cm^2, $\rho=2\times10^{10}$ cm^{-3}, $n_0=6\times10^8$, $z_0=3$ cm, $B=5$ s^{-1}, and a Zeeman shift of 3Γ cm^{-1}.

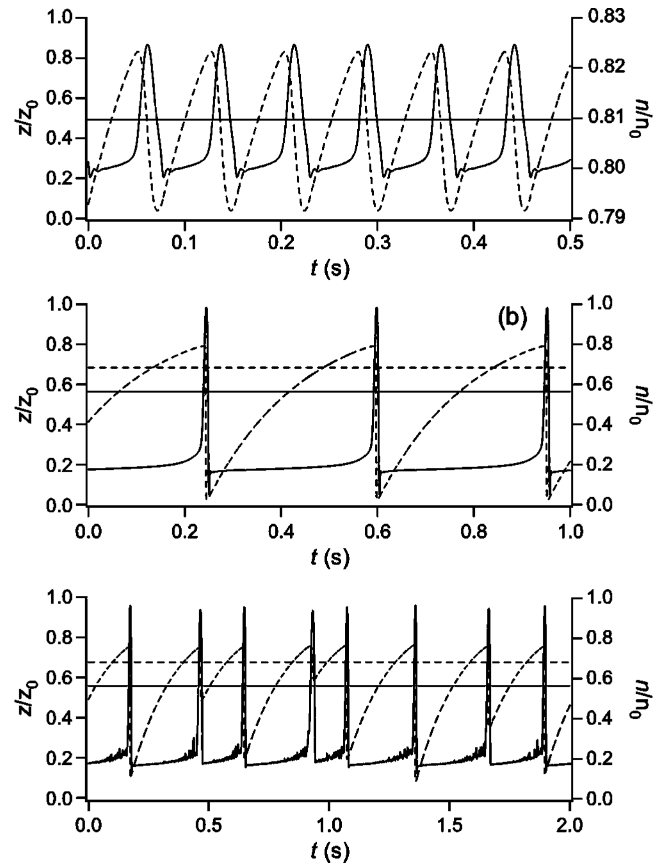

FIG. 5. Examples of the behavior of the cloud. The full (dashed) line curve is a plot of z (n) vs time. The horizontal full (dashed) line marks the stationary value z_s (n_s). In (a), $n_s/n_0=0.757$ is outside the figure. (a) shows a C_A instability for $\Delta_0=-0.37$; (b) shows a C_B instability for $\Delta_0=-0.35$; (c) corresponds to the same parameters as in (b), but a noise level of 7% has been added on I_1. Other parameters are the same as in Fig. 4.

in Ref. [6], with similar behaviors. We focus here on the area close to bistability, where the stationary solutions are unstable on the fold [Fig. 4]. For Δ_0 smaller than the fold, at the left of point H_1 on Fig. 4(a) ($\Delta_0<\Delta_{\mathrm{H}_1}$), the fixed point is a stable focus (F): the stationary solutions are stable and associated with an eigenfrequency ω_F decreasing with the detuning [Fig. 4(b)]. At the edge of the fold, the system exhibits a Hopf bifurcation (point H_1): the fixed point becomes a saddle focus (SF), and the stationary solutions become unstable. As Δ_0 is further increased, the eigenvalues become real at point P_1 [Figs. 4(a),4(b)], so that ω_F disappears and the fixed point becomes a saddle node (SN). Finally, when Δ_0 is still increased, the inverse sequence appears for the fixed point (SN$\rightarrow$SF$\rightarrow$ Hopf bifurcation $\rightarrow$F).

For $\Delta_0\gtrsim\Delta_{H_1}$, the stationary solution is unstable, but a stable periodic orbit appears in the vicinity of the fixed point, as is usual with a Hopf bifurcation. However, this orbit becomes unstable in the immediate neighborhood of H_1, while a homoclinic orbit appears, connecting the stable and unstable manifolds of the unstable fixed point. As Δ_0 is changed, the transition occurs through a complex sequence including period doubling, chaos, and multistability, on the interval $-0.402<\Delta_0<-0.400$. Such a complex sequence on such a narrow interval has of course no experimental meaning, and we do not expect to observe these dynamics in the experiment. The final regime, for $\Delta_0>-0.400$, is a cycle [Fig. 5(a)] with the characteristics of the C_A instabilities: the large amplitude is linked to its homoclinic origin, together with the low frequency. The appearance in the cycle of two stages with different characteristic times is due to the difference between the real part of the eigenvalues in the neighborhood of the bifurcation: during the slow stage, the system, leaving the fixed point, is governed by the positive eigenvalue, close to zero. In the fast stage, the system approaches the fixed point, following the stable manifold, associated with a large negative eigenvalue.

As the system is progressively carried off H_1, the trajectories leave the fixed point: for example, for $\Delta_0=-0.37$ [Fig. 5(a)], the trajectory is never in the vicinity of the fixed point, where the n_s coordinate is outside the graph. The shape gradually changes and the period decreases [Fig. 4(c)]. As the C_A behavior is not linked to the nature of the fixed point, it still exists in the SN zone, without any discontinuity at P_1 or P_2.

The amplitude of C_A is several millimeters when it appears at H_1, and increases regularly with Δ_0, so that in $\Delta_0\simeq-0.362$, the cloud border reaches z_0. At this point, the oscillation frequency abruptly decreases [Fig. 4(c)] and the shape of the limit cycle qualitatively changes. Indeed, the atoms beyond z_0 are lost, and so n can decrease rapidly. The resulting temporal behavior is still a periodic cycle and may be described as previously, except that the decrease of z is much faster and that of n is much larger [Fig. 5(b)]. It looks like the C_B experimental behavior, except that it is periodic. Note that this behavior is also observed in the F zone between H_2 and resonance: this means that a generalized bistability occurs between C_B and the stable stationary solution. This confirms that at this point, the periodic instabilities are no longer linked to the fixed-point properties.

To explain the difference between the C_B experimental and theoretical behaviors, we take into consideration the noise, which is known to play a fundamental role in this system [6]. Its influence on deterministic instabilities is well known: fixed points and limit cycles are usually robust with respect to noise, whose main effect is to shift slightly the bifurcation points [9]. So we do not expect to observe spectacular changes in the stationary and C_A behaviors when noise is added, and this is confirmed by the simulations. The C_B behavior is different, as, due to the border effects, the cloud could be very sensitive to noise in the vicinity of z_0: indeed, noise should induce large variations in the decreasing of n, and hence in the period of the dynamics. This is confirmed by the numerical simulations: Fig. 5(c) shows the behavior of the cloud for the same conditions as in Fig. 5(b), except that noise has been added to the trap intensity. As expected, the dynamics is no longer periodic, exhibiting large fluctuations in the return time, as observed in the experiment.

The simple model developed here allows us to understand the dynamical origin of the giant oscillations observed in the experiment. It is in good agreement with the experimental observation. The only difference concerns the detuning interval on which instabilities appear, which is one order of magnitude larger in the experiments. However, to make a real comparison, we should take into account the inevitable experimental variation of n_0 when Δ_0 is changed. Note that in the model, a simultaneous change of n_0 and Δ_0 leads to a relative stretch of the unstable zone. Unfortunately, as we have no simple way to establish experimentally the relation between n_0 and Δ_0, we are not able to check the amplitude of the correction in the present model.

In conclusion, we have demonstrated the existence of ''deterministic,'' in contrast to ''noise,'' instabilities in the MOT cloud. As a consequence, a simple amelioration of the experimental noise cannot improve the cloud stability. But mainly, this opens different perspectives in the characterization of the atomic systems. Indeed, it is well known that an unstable dynamics enables the experimental measure of more system parameters than in a stationary regime. The analysis of the dynamics of a perturbed MOT has already made possible the evaluation of the capture velocities [10]. The existence of periodic and chaotic dynamics in a MOT should enable the access to numerous other atomic quantities. It could be, for example, a way to find a signature of long-range interactions [11].

We thank J. Thywissen for his suggestions during the preparation of this paper. The Laboratoire de Physique des Lasers, Atomes et Molécules is ''Unité Mixte de Recherche de l'Université de Lille 1 et du CNRS'' (UMR 8523). The Centre d'Etudes et de Recherches Lasers et Applications (CERLA) is supported by the Ministère Chargé de la Recherche, the Région Nord–Pas de Calais, and the Fonds Européen de Développement Economique des Régions.

[1] F. Dalfovo *et al.*, Rev. Mod. Phys. **71**, 463 (1999).
[2] L. Guidoni *et al.*, Phys. Rev. A **60**, R4233 (1999); F.-R. Carminati *et al.*, Eur. Phys. J. D **17**, 249 (2001).
[3] B.G. Klappauf *et al.*, Physica D **131**, 78 (1999).
[4] See, e.g., Y. Sortais *et al.*, Phys. Rev. Lett. **85**, 3117 (2000), and references therein.
[5] G.K. Brennen *et al.*, Phys. Rev. Lett. **82**, 1060 (1999).
[6] D. Wilkowski *et al.*, Phys. Rev. Lett. **85**, 1839 (2000).
[7] See, e.g., Edward Ott, *Chaos in Dynamical Systems* (Cambridge University Press, Cambridge, U.K., 1993).
[8] D.W. Sesko *et al.*, J. Opt. Soc. Am. B **8**, 946 (1991).
[9] E. Arimondo *et al.*, in *Noise in Nonlinear Dynamical Systems*, edited by F. Moss and P. V. E. McClintock (Cambridge University Press, Cambridge, U.K., 1989), Vol. III.
[10] D. Wilkowski *et al.*, Eur. Phys. J. D **2**, 157 (1998).
[11] R. Kaiser (private communication).